Metabolic Engineering 79 (2023) 27–37

Contents lists available at ScienceDirect

Metabolic Engineering

journal homepage: www.elsevier.com/locate/meteng

Laboratory evolution of *Synechocystis* sp. PCC 6803 for phenylpropanoid production

Kateryna Kukil [a], Elias Englund [b], Nick Crang [b], Elton P. Hudson [b], Pia Lindberg [a,*]

[a] Microbial Chemistry, Department of Chemistry - Ångström, Uppsala University, Box 523, SE 751 20, Uppsala, Sweden
[b] School of Engineering Sciences in Chemistry, Biotechnology and Health, Science for Life Laboratory, KTH – Royal Institute of Technology, Stockholm, Sweden

ARTICLE INFO

Keywords:
Synechocystis PCC 6803
Aromatic amino acids
Laboratory evolution
Trans-cinnamic acid
p-coumaric acid

ABSTRACT

Cyanobacteria are promising as a biotechnological platform for production of various industrially relevant compounds, including aromatic amino acids and their derivatives, phenylpropanoids. In this study, we have generated phenylalanine resistant mutant strains (PRMs) of the unicellular cyanobacterium *Synechocystis* sp. PCC 6803, by laboratory evolution under the selective pressure of phenylalanine, which inhibits the growth of wild type *Synechocystis*. The new strains of *Synechocystis* were tested for their ability to secrete phenylalanine in the growth medium during cultivation in shake flasks as well as in a high-density cultivation (HDC) system. All PRM strains secreted phenylalanine into the culture medium, with one of the mutants, PRM8, demonstrating the highest specific production of 24.9 ± 7 mg L^{-1}·OD_{750}^{-1} or 610 ± 196 mg L^{-1} phenylalanine after four days of growth in HDC. We further overexpressed phenylalanine ammonia lyase (PAL) and tyrosine ammonia lyase (TAL) in the mutant strains in order to determine the potential of PRMs for production of *trans*-cinnamic acid (*t*CA) and *para*-coumaric acid (*p*Cou), the first intermediates of the plant phenylpropanoid pathway. Productivities of these compounds were found to be lower in the PRMs compared to respective control strains, except for PRM8 under HDC conditions. The PRM8 background strain in combination with PAL or TAL expression demonstrated a specific production of 52.7 ± 15 mg L^{-1}·OD_{750}^{-1} *t*CA and 47.1 ± 7 mg L^{-1}·OD_{750}^{-1} *p*Cou, respectively, with a volumetric titer reaching above 1 g L^{-1} for both products after four days of HDC cultivation. The genomes of PRMs were sequenced in order to identify which mutations caused the phenotype. Interestingly, all of the PRMs contained at least one mutation in their *ccmA* gene, which encodes DAHP synthase, the first enzyme of the pathway for aromatic amino acids biosynthesis. Altogether, we demonstrate that the combination of laboratory-evolved mutants and targeted metabolic engineering can be a powerful tool in cyanobacterial strain development.

1. Introduction

Secondary plant metabolites such as phenylpropanoids, have been used over centuries as flavoring agents and colorants and for treating human diseases due to their bioactive properties (Rao and Ravishankar 2002, Ververidis et al., 2007). Microbial synthesis of these plant metabolites is a highly promising alternative to the traditional extraction from natural sources or chemical synthesis methods, which may not be sustainable or are too inefficient for commercial production. Among microbial hosts, cyanobacteria can be used as a truly sustainable platform where target molecules are synthesized by direct conversion of CO_2.

Successful heterologous production of starting compounds of the phenylpropanoid pathway from the aromatic amino acids phenylalanine (Phe) and tyrosine (Tyr) was already demonstrated in the model cyanobacterial strain *Synechocystis* sp. PCC 6803 (hereafter *Synechocystis*) (Brey et al., 2020; Deshpande et al., 2020; Gao et al., 2021; Kukil and Lindberg 2022). However, the titers of the desired molecules produced in cyanobacteria still need to be enhanced to enable large scale production.

Abbreviations: PRM, phenylalanine resistant mutant strain; HDC, high-density cultivation; *Synechocystis*, *Synechocystis* sp. PCC 6803; PAL, phenylalanine ammonia lyase; TAL, tyrosine ammonia lyase; *t*CA, *trans*-cinnamic acid; *p*Cou, *para*-coumaric acid; Phe, phenylalanine; Tyr, tyrosine; DAHP, 3-deoxy-d-arabinoheptulosonate-7-phosphate synthase; DAHPS, DAHP synthase; *E. coli*, *Escherichia coli*; EVC, empty vector control.

* Corresponding author.
E-mail address: pia.lindberg@kemi.uu.se (P. Lindberg).

https://doi.org/10.1016/j.ymben.2023.06.014
Received 20 April 2023; Received in revised form 14 June 2023; Accepted 29 June 2023
Available online 29 June 2023

Phenylpropanoids are solely derivatives of the central pathway of aromatic amino acids synthesis, the shikimate pathway (Yadav et al., 2020). In cyanobacteria, this pathway is understudied as compared to other microbial hosts, which makes rational pathway engineering challenging. The pathway starts from the condensation of erythrose 4-phosphate and phosphoenolpyruvate into the first compound 3-deoxy-d-arabinoheptulosonate-7-phosphate (DAHP) by the enzyme DAHP synthase (DAHPS) (Fig. 1). Through six consecutive reactions, DAHP undergoes cyclisation to form chorismate, which is a precursor not only for all three aromatic amino acids Phe, Tyr and tryptophan, but also for folate, phylloquinone, plastoquinone, molybdopterin as well as tocopherols and carotenoids (Sprenger 2006). The majority of the enzymes of shikimate pathway have high sequence similarity between *Escherichia coli* (*E. coli*) and *Synechocystis*, with some exceptions. For instance, the fourth enzyme, shikimate dehydrogenase, is not annotated for *Synechocystis* in KEGG (https://www.genome.jp/kegg/) and no sequences with homology to this enzyme can be found in the *Synechocystis* genome sequence. Furthermore, the step of arogenate synthesis from prephenate, prephanate aminotransferase (PAT) has not yet been identified.

Additionally, very little is known about the native regulation of the shikimate pathway in *Synechocystis*. Usually, the production of aromatic amino acids is controlled by the demands via allosteric feedback regulation of multiple enzymes by the end products of the pathway. The first enzyme, DAHPS, plays a crucial role for this control in many different studied organisms (Jiao 2021). In an early study by Hall and Jensen (1980) on *Synechocystis* sp. 29108, it was demonstrated that growth inhibition by Phe can be attributed to the sensitivity of DAHPS to inhibition by Phe, resulting in downregulation of this enzyme and subsequent lack of Tyr and tryptophan. In their experimental setup, the authors used 2-fluoro and 4-fluoro derivatives of Phe as selective agents to obtain phenylalanine resistant mutants (PRM). The mutant strains were also secreting Phe and Tyr, possibly due to relieved Phe inhibition of mutated DAHPS.

Another early study of Labarre et al. (Labarre et al., 1987) on amino acid transporters in *Synechocystis* acquired a similar kind of resistant mutants. In their study, in order to determine active transport systems involved in amino acids uptake, cells were grown with toxic amino acids and analogues (4-azaleucine, histidine, or *para*-fluorophenylalanine and α-methyl-*p*-tyrosine) until resistant mutants spontaneously appeared. The group of mutants resistant to *para*-fluorophenylalanine as well as to Phe and α-methyl-*p*-tyrosine were also strong overproducers of Phe and Tyr. As suggested by the authors, these mutants were likely to be regulatory mutants of the aromatic amino acids biosynthesis.

We found it interesting that in both studies these spontaneous mutants while being resistant to toxic analogues of Phe were also secreting Phe and Tyr. In recent studies, the production of aromatic amino acids has been accomplished only by certain genetic manipulations (Brey et al., 2020). Compared to the common approach of direct genetic engineering in order to make an organism produce aromatic compounds, the same was achieved in the earlier studies by spontaneous mutation(s) under selective metabolic pressure. Furthermore, Deshpande et al. (Deshpande et al., 2020) recently demonstrated in a study on tryptophan production in *Synechocystis*, that the combination of metabolic engineering and random mutagenesis approaches is a successful strategy superior to either approach alone.

In this study, we aimed to adapt the methods from studies of Hall and Jensen (1980) and Labarre et al., (1987) for laboratory evolution as an alternative approach to direct genetic engineering to obtain resistant *Synechocystis* mutants able to produce aromatic amino acids. Instead of using toxic amino acids analogues as selective pressure, we used Phe, since as demonstrated already, its concentration in the growth media

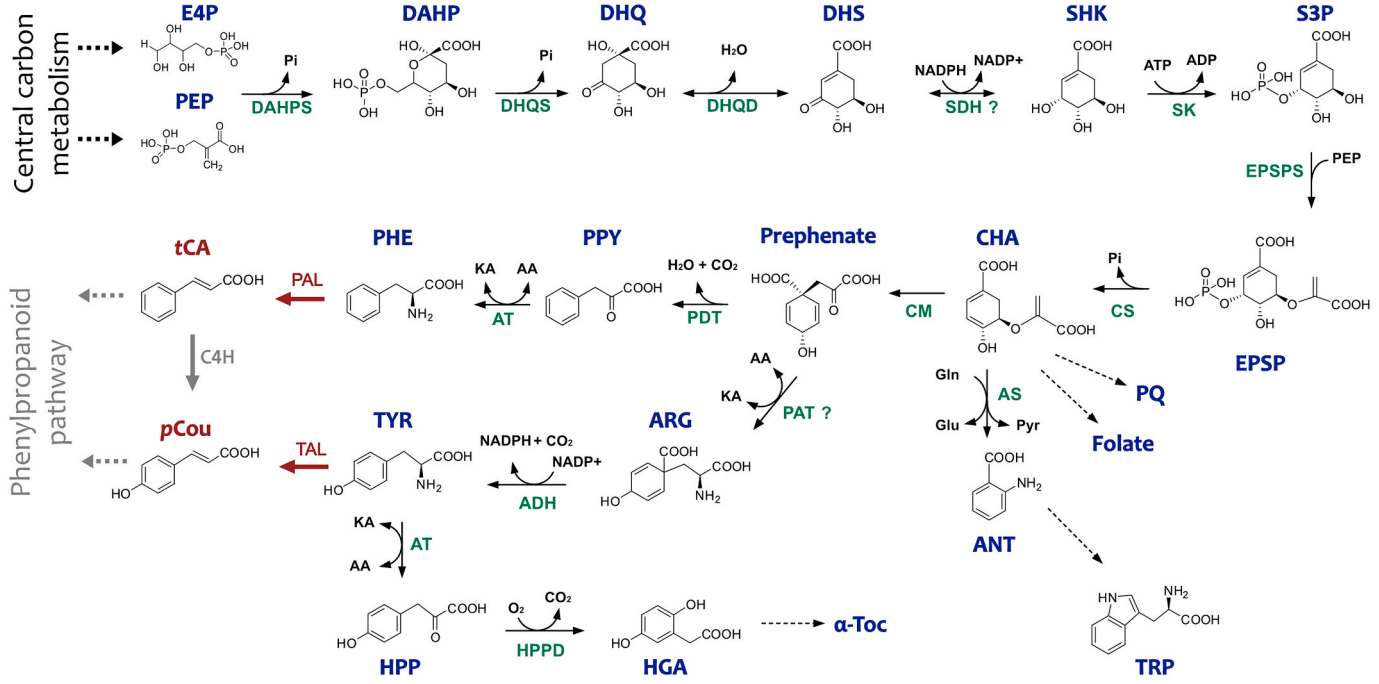

Fig. 1. Schematic overview of Shikimate pathway for biosynthesis of aromatic amino acids in cyanobacteria. Compounds and enzymes not present in *Synechocystis* are highlighted in red and grey color. Question marks correspond to the not identified enzymes or enzymes with no homology in *Synechocystis*. Abbreviations: ARG, arogenate; ANT, anthranilate; CHA, chorismate; DAHP, 3-deoxy-D-arabinoheptulosonate 7-phosphate; DHQ, 3-dehydroquinate; DHS, 3-dehydroshikimate; E4P, erythrose-4-phosphate; EPSP, 5-enolpyruvylshikimate 3-phosphate; HGA, homogentisate; HPP, 4-hydroxyphenylpyruvate; *p*Cou, *para*-coumaric acid; PEP, phosphoenolpyruvate; PHE, L-phenylalanine; PPY, phenylpyruvate; PQ, plastoquinone; S3P, shikimate-3-phosphate; SHK, shikimate; *t*CA, *trans*-cinnamic acid; TRP, L-tryptophan; TYR, L-tyrosine. Enzymes: ADT, arogenate dehydrogenase; AS, anthranilate synthase; AT, aminotransferase; C4H, cinnamate-4-hydroxylase; CM, chorismate mutase; CS, chorismate synthase; DAHPS, 3-deoxy-D-arabinoheptulosonate 7-phosphate synthase; DHQD, 3-dehydroquinate dehydrogenase; DHQS, 3-dehydroquinate synthase; EPSPS, 5-enolpyruvylshikimate 3-phosphate synthase; HPPD, 4-hydroxyphenylpyruvate dioxygenase; PAL, phenylalanine ammonia lyase; PAT, prephenate aminotransferase; PDT, prephenate dehydratase; SDH, shikimate dehydrogenase; SK, shikimate kinase; TAL, tyrosine ammonia lyase.

above 0.1 mM (16.5 mg L^{-1}) inhibits the growth (Hall and Jensen 1980). Ten mutant strains were selected and all of them, unlike wild type (WT), were secreting Phe in the growth media, reaffirming the possibility to utilize this method of metabolite selective pressure for strain development. Further, we overexpressed phenylalanine ammonia lyase (PAL) and tyrosine ammonia lyase (TAL) derived from our previous study (Kukil and Lindberg 2022) in the PRMs in order to evaluate the potential for production of the phenylpropanoid precursors *trans*-cinnamic acid (*t*CA) and *para*-coumaric acid (*p*Cou) in these new strains. The genomes of three PRMs were sequenced with Illumina NextSeq platform in order to identify mutations which could cause the phenotype. The metabolic mutants obtained in this study represent an extremely interesting material for understanding and engineering the aromatic amino acids metabolism in cyanobacteria.

2. Materials and methods

2.1. Bacterial strains and growth conditions

In this study, a glucose-tolerant model unicellular cyanobacterium *Synechocystis* sp. PCC 6803 was used. Cultures of *Synechocystis* were grown at 30 °C under constant 45 μmol photons m^{-2} s^{-1} light intensity in BG11 medium (Stanier and Cohen-Bazire 1977) with addition of kanamycin (Km) at a final concentration 25 μg ml^{-1}. For the growth experiment with Phe supplementation, a 16.5 g L^{-1} (100 mM) stock of Phe in BG11 was filter-sterilized though 0.2 μm pore cellulose filters (VWR) and added in aliquots to yield approximate millimolar concertation desired in the final culture volume. Small-scale high-density cultivation experiments were performed in 10 mL scale using HD10 cultivators (CellDEG, GmbH) as described previously (Kukil and Lindberg 2022). *Escherichia coli* DH5 αZ1 (Invitrogen) used for conjugation were grown in LB medium at 37 °C, supplemented with Km antibiotic to the final concentration in the medium 50 μg ml^{-1} (Sigma, Merck).

2.2. Selection of Synechocystis mutants

The procedure of spontaneous mutant selection was similar to what was described previously (Hall and Jensen 1980, Labarre et al., 1987). Exponentially grown *Synechocystis* culture (OD_{750} ~0.3) were concentrated by centrifugation and spread onto buffered BG11 plates supplemented with 165 mg L^{-1} (1 mM) of Phe. Resistant colonies appeared after 5–7 days of incubation at 30 °C. Each colony was then transferred into 24-well plate with liquid BG11 medium containing 165 mg L^{-1} (1 mM) Phe. Cultures that gained yellow color were discarded and those that remained green in the liquid cultures were re-inoculated in the 6-well plate BG11 media with increased concentration of Phe. The rounds of selection finished when the remaining cultures were able to grow at 1.98 g L^{-1} (12 mM) Phe in the media.

2.3. Conjugation of Synechocystis

Obtained *Synechocystis* resistant mutants were transformed by conjugation with *At-pal*-pEEK and *Ts-pal*-pEEK plasmids carrying PAL from *Arabidopsis thaliana* and TAL from *Treponema socranskii* subsp. *paredis ATCC 35535,* correspondingly, under the control of Ptrc RBS* in pEEK which were constructed in our previous study (Kukil and Lindberg 2022). Conjugation was performed as described previously (Kukil and Lindberg 2022). In order to determine relative PAL and TAL protein expression in engineered strains, the soluble protein fraction was extracted from *Synechocystis* cells as described by Ivleva and Golden (2007) (Ivleva and Golden 2007). Proteins were separated by SDS-PAGE, using Mini-PROTEAN TGX™ gels (Bio-Rad), and transferred to a PVDF membrane (Bio-Rad). Immunoblot was performed according to standard techniques using Anti-Strep-tag II (Abcam) for the detection of Strep-tagged proteins.

2.4. Determination of Phe, tCA and pCou

Determination of Phe, *t*CA and *p*Cou in the growth media was performed by LC-MS. For this 1 ml of supernatant was taken from *Synechocystis* cultures, samples were filtered through 0.2 μm pore PTFE filters (Fisherbrand) and subjected to HPLC analysis. Samples were stored at −20 °C if not analyzed the same day. HPLC-MS analysis was performed using an Agilent 1290 Infinity II HPLC system equipped with a 1290 Infinity II High Speed pump and a 1260 II Infinity DAD HS UV–vis detector, using an InfinityLab POROSHELL SB-120 C18 column with dimensions of 100mm × 2.1 mm and 2.7 μm particle size. The HPLC was coupled to an InfinityLab LC/MSD equipped with an ESI source as ionization. LC separation was performed using a water (A, 0.1% formic acid) and acetonitrile (B) eluent system using the method: 0–1 min 10% B; 1–10 min 10 → 90% B; 10–11 min 90% B; 11–11.1 min 90-10% B, 11.1–12 min 10% B; at the flow rate of 0.3 ml/min. The quantification of *t*CA and *p*Cou in *Synechocystis* cultures was based on a linear calibration curve from standards measured in technical triplicates. For Phe quantification, the area of total ion chromatogram was used. Standards for corresponding compounds (Sigma, Merck) were prepared in BG11 medium in the range 1–100 μg ml^{-1} and filtered before analysis.

2.5. DNA sequencing

Genomic DNA was extracted by phenol-chloroform extraction as described previously (Tamagnini et al., 1997). For whole genome sequencing, a 500 ng aliquot of genomic DNA was suspended in 15 μL of 10 mM Tris buffer, placed in a microTUBE-15 AFA Beads tube (Covaris) and fragmented into 300 bp fragments using an ME220 focused ultrasonicator (Covaris). Fragment end repair and adaptor ligation was performed using an NEBNext Ultra II DNA Library Prep Kit (New England Biolabs) following the manufacturer's protocol. Size selection of NEB adaptor ligated fragments was carried out using SPRISelect magnetic beads (Beckman Coulter) following the method in the NEBNext Ultra II DNA Library Prep Kit User manual. Illumina adaptors and indexes for demultiplexing were added via PCR using NEBNext Multiplex Oligos for Illumina (New England Biolabs). PCR products were separated on a 1% agarose gel and gel extraction was performed on the band between 300 and 600 bp using a Gel Extraction Kit (ThermoScientific). The DNA concentration of the samples were quantified using a Qubit dsDNA HS Assay Kit (Invitrogen). The sample was sequenced as part of a mixed pool using a NextSeq 1000/2000 P2 reagents (100 Cycles) v3 kit, (Illumina) run on a NextSeq 1000 instrument (Illumina) according to the manufacturer's instructions. Library loading concentration was 650 pM with a 1% phiX spike. Loci of *sll0934*, *slr1916* and *sll1995* genes from remaining PRMs were amplified using corresponding primer pairs and sent for sequencing (Eurofins Genomics) using same primers as for the amplification.

3. Results and discussion

3.1. Growth inhibition of Synechocystis by phenylalanine

To assess the impact of external Phe on *Synechocystis* growth, we first used an empty vector control strain (EVC), obtained in a previous study (Kukil and Lindberg 2022) (see Table 1 for list of strains used in this study). We grew this strain in medium supplemented with different concentrations of Phe. The presence of Phe in the medium inhibited the growth of *Synechocystis* (Fig. 2A) and the inhibited cell cultures turned yellow, similar to what was observed previously (Hall and Jensen 1980). This is likely due to inhibition of DAPHS that results in starvation for Tyr and tryptophan and subsequently decreased phycocyanin content causing the yellow coloration. However, as shown in Fig. 2A, the growth of the cultures was restored over time. We monitored the Phe concentration in the growth medium to see if the externally provided Phe was

Table 1
List of *Synechocystis* strains used in this study.

Strain	Comment	Antibiotic resistance	Reference
EVC	Empty vector control strain of *Synechocystis* WT harboring pEEK* plasmid for Km resistance	Km	(Kukil and Lindberg 2022)
AtC	Based *Synechocystis* WT harboring *Arabidopsis thaliana* PAL expressed from P*trc* RBS* in pEEK	Km	(Kukil and Lindberg 2022)
TsC	Based *Synechocystis* WT harboring *Treponema socranskii* TAL expressed from P*trc* RBS* in pEEK	Km	(Kukil and Lindberg 2022)

Strains based on spontaneous resistant mutants obtained in this study

Name	Comment	Name	Comment	Antibiotic resistance
AtPRM1	Same as PRM1, but carries *At-pal*-pEEK	**TsPRM1**	Same as PRM1, but carries *Ts-tal*-pEEK	Km
AtPRM3	Same as PRM3, but carries *At-pal*-pEEK	**TsPRM3**	Same as PRM3, but carries *Ts-tal*-pEEK	Km
AtPRM4	Same as PRM4, but carries *At-pal*-pEEK	**TsPRM4**	Same as PRM4, but carries *Ts-tal*-pEEK	Km
AtPRM5	Same as PRM5, but carries *At-pal*-pEEK	**TsPRM5**	Same as PRM5, but carries *Ts-tal*-pEEK	Km
AtPRM6	Same as PRM6, but carries *At-pal*-pEEK	**TsPRM6**	Same as PRM6, but carries *Ts-tal*-pEEK	Km
AtPRM7	Same as PRM7, but carries *At-pal*-pEEK	**TsPRM7**	Same as PRM7, but carries *Ts-tal*-pEEK	Km
AtPRM8	Same as PRM8, but carries *At-pal*-pEEK	**TsPRM8**	Same as PRM8, but carries *Ts-tal*-pEEK	Km
AtPRM10	Same as PRM10, but carries *At-pal*-pEEK	**TsPRM10**	Same as PRM10, but carries *Ts-tal*-pEEK	Km
AtPRM11	Same as PRM11, but carries *At-pal*-pEEK	**TsPRM11**	Same as PRM11, but carries *Ts-tal*-pEEK	Km
AtPRM12	Same as PRM12, but carries *At-pal*-pEEK	**TsPRM12**	Same as PRM12, but carries *Ts-tal*-pEEK	Km

consumed by the time when culture growth recovered. The results show that the supplemented Phe was not consumed (Fig. 2C), indicating that growth recovery is a result of appearance of resistant cells. The timing of the emergence of resistant cells depends on the dosage of externally provided Phe, with lower concentration facilitating it faster. It is interesting to consider what molecular mechanisms are underlying this adaptation process, as it appears that the cell division was strongly impaired during Phe inhibition. This difference in timing depending on supplied Phe concentration may reflect that a larger number of individual mutations are required for the cells to cope with higher concentration of Phe.

To check whether the expression of heterologous PAL can relieve the inhibitory effect of Phe by converting it into *t*CA, we next tested a strain of *Synechocystis*, which expresses PAL from *Arabidopsis thaliana* (AtC, see Table 1) (Kukil and Lindberg 2022). The AtC strain showed growth inhibition only at the highest Phe concentrations tested, at approximately 0.66 or 1.65 g L^{-1} (4 or 10 mM) Phe. However, no clear indication of resistant cells appearing was observed after 14 days of cultivation with these concentrations, apart from a slight recovery of growth at days 8–10 (Fig. 2B). In the growth medium of AtC cultures, all the Phe supplemented at concentrations of approximately 16.5 and 165 mg L^{-1} (0.1 and 1 mM) was converted into *t*CA (Fig. 2D). Accumulation of *t*CA and decrease of Phe was observed in the cultures with the highest concentrations of Phe, however, it seems that the Phe inhibition was dominating over the effect of the PAL activity, and thus the culture growth was suppressed until slight growth improvement after the 10th day was observed (Fig. 2B).

The transport of amino acids in *Synechocystis* includes specific transporters for basic, neutral and acidic amino acids (Labarre et al., 1987; Quintero et al., 2001). However, the role of these transporters is primarily in recapturing of amino acids that have leaked out from the cell. Thereby, the "intake-only" operation mode of the amino acid transporters could explain the Phe growth inhibition effect: externally provided Phe will be captured by cells despite that it leads to growth impairment. Based on our measurements of the Phe concentration in the media, where Phe concentration decrease after 14 days was ~7 mg L^{-1} (Fig. 2C, data from approximately 16.5 mg L^{-1} (0.1 mM) Phe), it also seems that the amount of consumed Phe which causes growth impairment is extremely low.

3.2. Laboratory evolution of wild type Synechocystis

To generate PRMs of *Synechocystis*, WT cells were spread on BG11 agar plates supplemented with 165 mg L^{-1} (1 mM) Phe. When spontaneous resistant colonies appeared, individual colonies were picked up and transferred into liquid medium with 165 mg L^{-1} (1 mM) Phe. After 3–5 days of growth under constant low light intensity, cell cultures that remained green were re-inoculated into fresh BG11 medium with increased Phe concentration. The re-inoculation cycles were repeated several times until the growth of remaining cultures was not affected by presence of 1.98 mg L^{-1} (12 mM) Phe in the growth medium. Following this procedure, we have isolated ten Phe resistant mutants (PRM1-12). The isolated PRMs showed no growth inhibition when cultivated in BG11 medium supplemented with 330 mg L^{-1} (2 mM) Phe, unlike the WT control strain (Fig. S1), confirming the stability of the phenotype. Secreted Phe was measured during shake flasks cultivation of PRMs under medium light intensity in standard BG11 medium (Fig. 3A). The productivity of several PRMs was nearly similar, reaching a volumetric titer of about 26 mg L^{-1} of Phe for PRM3 and PRM5 after eight days, with the highest specific titer of 9.1 ± 0.7 mg $L^{-1}\cdot OD_{750}^{-1}$ reached for PRM10 (Fig. 3A, Table S1). Notably, PRM12 demonstrated the lowest productivity and no Phe was detected on day 4 of the growth experiment, indicating that this PRM gained different mutations compared to others. Tyr was detected in the growth medium in all PRMs, however the concentration was too low to quantify. Interestingly, the growth of PRMs, except PRM8 and PRM12, was similar compared to the WT (Fig. 3B). Analogous observations were made for the tryptophan overproducer mutant of *Synechocystis* (Deshpande et al., 2020) as well as sucrose overproducing *Synechococcus elongatus* (Ducat et al., 2012), indicating that the presence of an additional electron sink has a positive effect on the photosynthetic productivity in *Synechocystis* (Grund et al., 2019).

To further explore the potential of Phe production by PRMs, we tested their productivity with small-scale high-density cultivation (HDC). The HDC cultivation system from CellDEG (www.celldeg.com) has been successfully used previously to demonstrate high production rates in a short time period for various compounds in cyanobacteria (Lippi et al., 2018, Dehm et al., 2019, Dienst et al., 2020, Moschny et al., 2020; Rodrigues and Lindberg 2021; Kukil and Lindberg 2022). A set of PRMs with distinct characteristics were tested under HDC conditions. The specific Phe productivity was similar or lower in HDC cultures than in the shake flask cultivation for all tested PRMs except PRM8 (Fig. 4A). For PRM8, the production was 6 times or more higher compared to the other PRMs, and the titer reached 24.9 ± 7 mg $L^{-1}\cdot OD_{750}^{-1}$ or 610 ± 196 mg L^{-1} after 4 days of high-density cultivation. Unlike under standard cultivation conditions, PRM8 demonstrated growth similar to WT and only PRM12 retained slower growth rate than WT (Fig. 4B).

As suggested previously, the secretion of Phe by spontaneous resistant strains may be due to insensitivity of DAHPS to inhibition by Phe, which was gained after the selection on Phe or toxic analogues (Hall and

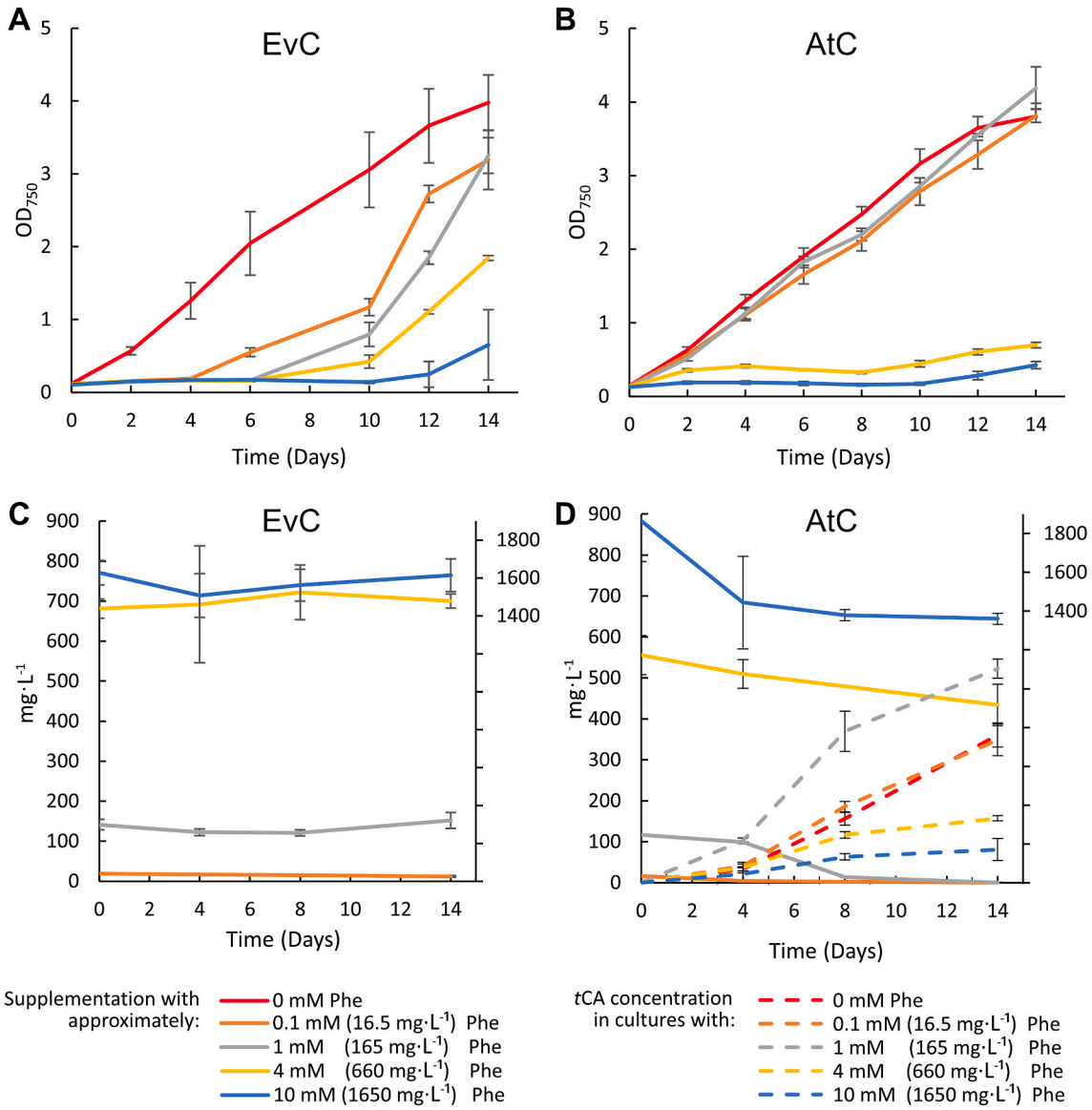

Fig. 2. Growth of the empty vector control EVC (**A**) and PAL-expressing AtC (**B**) strains with addition of various phenylalanine concentrations during 14 days under constant 45 µmol photons m^{-2} s^{-1} light intensity. Concentration of phenylalanine in the growth medium of EVC (**C**) and AtC (**D**) cultures. Note that data from growth experiments of cultures with 10 mM Phe in panels C and D are displayed on the secondary axes on the right, for better visualization of the values. Error bars represent standard deviation of the biological replicates.

Jensen 1980). According to this scenario, Phe or its analog would no longer bind and inhibit activity of the first enzyme of the shikimate pathway, which would result in an accumulation of the pathway end products. Indeed, overexpression of feedback-inhibition-resistant versions of DAHPS and chorismate mutase/prephenate dehydrogenase from *E. coli* leads to Phe and Tyr accumulation in *Synechocystis* (Brey et al., 2020), and thereby the secretion of Phe might be a result of high Phe synthesis rates combined with a comparatively slow uptake of amino acids by transport systems. However, the different Phe secreting mutants we obtained in this study demonstrate distinct results regarding Phe accumulation during HDC, in particular in PRM8 compared to other strains. This indicates that the variants may have acquired not only DAHPS insensitivity, but some other mutation(s) as well. It is also possible, that the secreted Phe is consumed again by the cells during the growth under high-density cultivation conditions, due to the high demand of proteinogenic amino acids for rapid culture growth and biomass synthesis, especially at the beginning of the growth experiment. During the first two days of cultivation, the cell density increased 25-50 times, while from day two to day four the increase in OD_{750} was about four times. This is consistent with the specific Phe production which was 5–20 times lower on day 2 compared to day 4. To test the hypothesis that lower or similar titers in HDC compared to shake flask cultures are due to the re-uptake of secreted Phe from the medium, we performed an additional HDC experiment, where on the second day of cultivation, 1 ml of 100 mM Phe stock was added to the cultures, resulting in a concentration of about 1.65 g L^{-1} (10 mM) Phe. The results in Fig. 5A show that indeed, the supplemented Phe concentration was decreased in WT and PRM1 cultures, possibly due to consumption by the cells. In case of PRM8, however, Phe titer was increased from day two till day four. Interestingly, during standard shake flask cultivation, a similar concentration of Phe completely inhibited the growth of the EVC until resistant cells appeared on day 12 (Fig. 2A), while during HDC the growth of WT *Synechocystis* was only slightly decreased (Fig. 5B) and external Phe was partially incorporated (Fig. 5A). Possibly, the high OD_{750} (~5) on day two when Phe was added could have diminished the inhibitory effect on the WT strain. Altogether, the decrease of specific

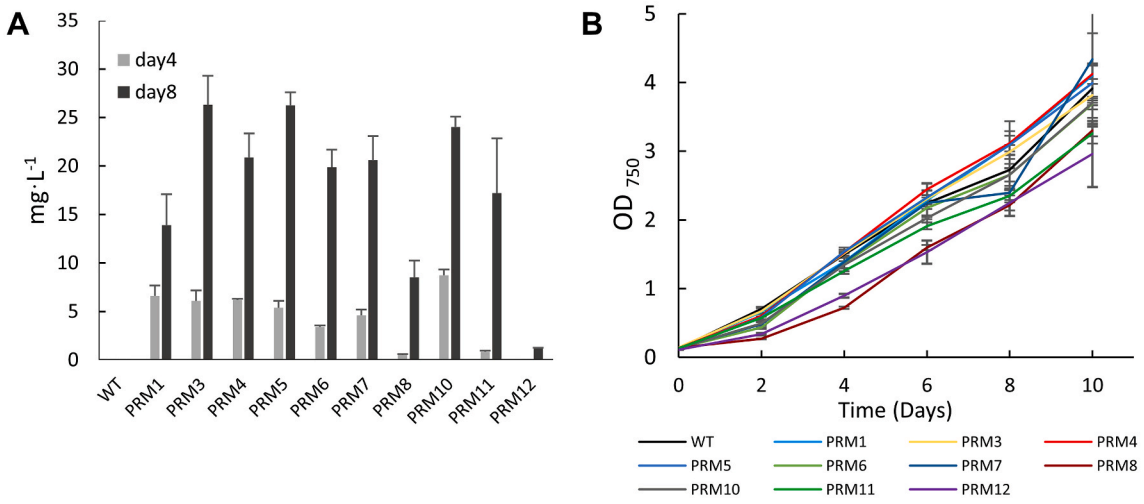

Fig. 3. Productivity and growth of PRMs during shake flasks cultivation. **A** Comparison of phenylalanine production in ten PRM variants and WT. Samples were taken from the growth medium at day four and day eight. The values are the means of three biological replicates and two technical replicates, error bars represent the standard deviation between biological replicates. **B** Growth curves of WT and PRMs during ten days. Error bars represent standard deviation between biological replicates.

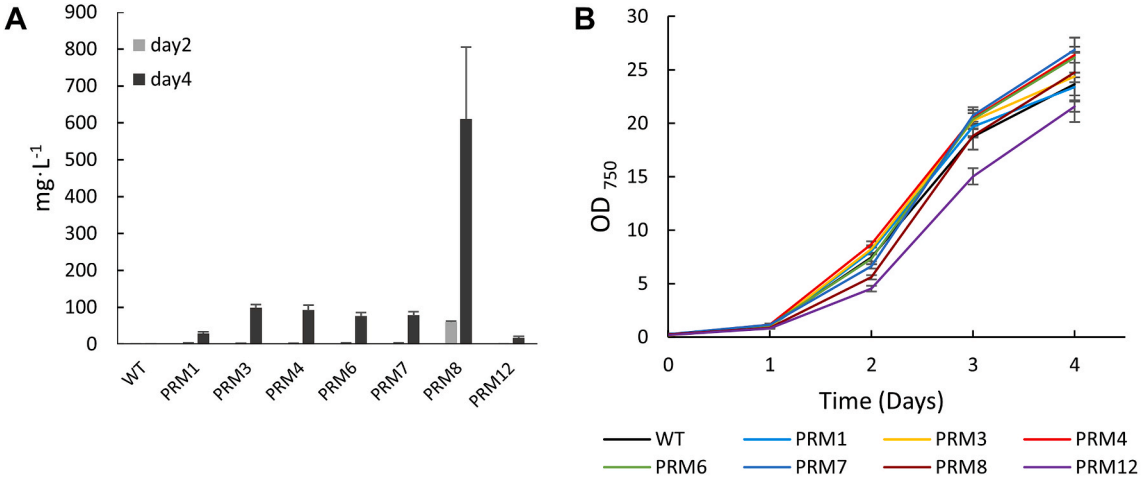

Fig. 4. Productivity and growth of PRMs during high-density cultivation. A Comparison of phenylalanine production in seven selected PRM variants and WT. Samples were taken from the growth medium at day two and day four. The values are the means of three biological replicates and two technical replicates, error bars represent the standard deviation of three biological replicates. **B** Growth curves of WT and PRMs during 4 days. Error bars represent standard deviation.

production rate of PRMs during high-density cultivation compared to shake flasks experiment might be a result of the re-uptake of secreted Phe.

3.3. Overexpression of PAL and TAL in PRMs background

As the next step, we aimed to use the Phe-secreting PRMs for the production of *t*CA and *p*Cou, the starting intermediates of the plant phenylpropanoids pathway (Vogt 2010), by overexpressing PAL or TAL enzymes correspondingly (see Fig. 1). *t*CA and *p*Cou are not metabolized by *Synechocystis* cells and thus can create an additional heterologous sink, whereas the deregulation of the shikimate pathway in PRMs could result in the increased productivity of these compounds as demonstrated by Brey et al. by expression of feedback resistant DAHPS (Brey et al., 2020). In a previous study (Kukil and Lindberg 2022), we tested the expression of several PAL and TAL enzymes in *Synechocystis,* where the highest specific titer of respective acid was obtained by strains expressing PAL from *Arabidopsis thaliana* and TAL from *Treponema socranskii*, and we therefore chose these enzymes for expression in the PRM strains.

Ten PRMs were successfully conjugated with self-replicative vectors carrying *At*PAL from *Arabidopsis thaliana* or *Ts*TAL from *Treponema socranskii* under the control of a constitutive promoter, resulting in the series of strains AtPRM1-12 and TsPRM1-12, respectively (Table 1). However, during photoautotrophic growth in shake flasks, the production of *t*CA and *p*Cou was lower in the PRM backgrounds compared to the respective *At* PAL and *Ts* TAL expressing WT background strains, AtC and TsC (Fig. 6 A and C). Relative PAL and TAL abundance was similar in all engineered strains (Fig. S2). The ten AtPRM variants demonstrated similar levels of specific *t*CA accumulation, which is a nearly two-fold decreased compared to the control strain. The productivity of *p*Cou in the PRM background strains was also lower than in the TsC control strain, but to a lesser extent, and with exception of TsPRM8. Both TsC and TsPRM8 reached a similar titer of *p*Cou of 24 mg L^{-1}·OD_{750}^{-1} after eight days of cultivation. The growth of AtPRM and TsPRM variants was similar to the respective control strain, AtC and TsC (Fig. 6C and D). Notably, PRM12, which showed the lowest Phe productivity (Fig. 3A), when overexpressing PAL or TAL demonstrated a specific productivity of

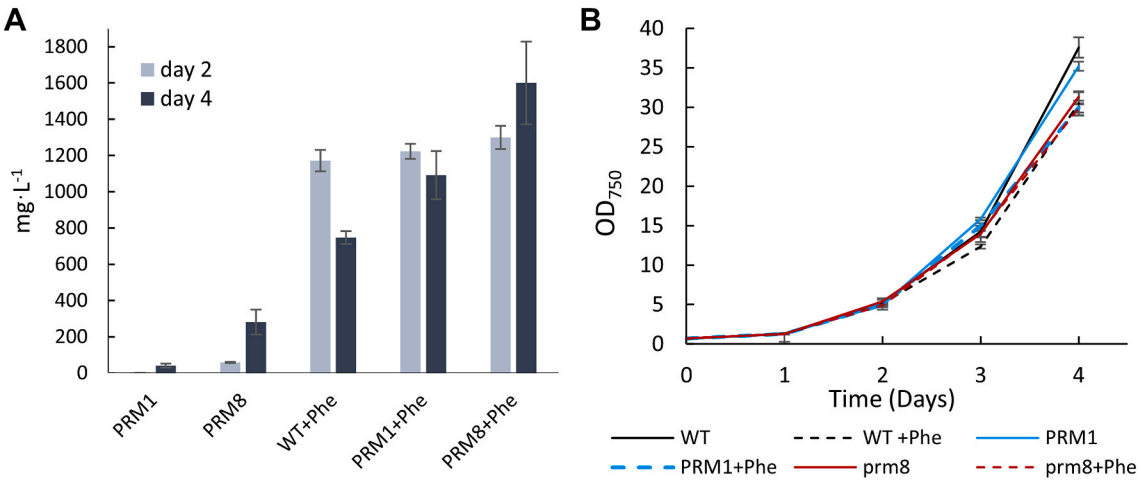

Fig. 5. Effect of Phe supplementation of growth and Phe uptake on *Synechocystis* WT, PRM1 and PRM8 strains during HDC. Phe was added on day two. **A** Concentration of Phe in media of WT and PRM cultures with and without Phe addition. **B** Growth curves of WT, PRM1 and PRM8 during four days of cultivation. The values are the means of three biological replicates and two technical replicates, error bars represent the standard deviation of three biological replicates.

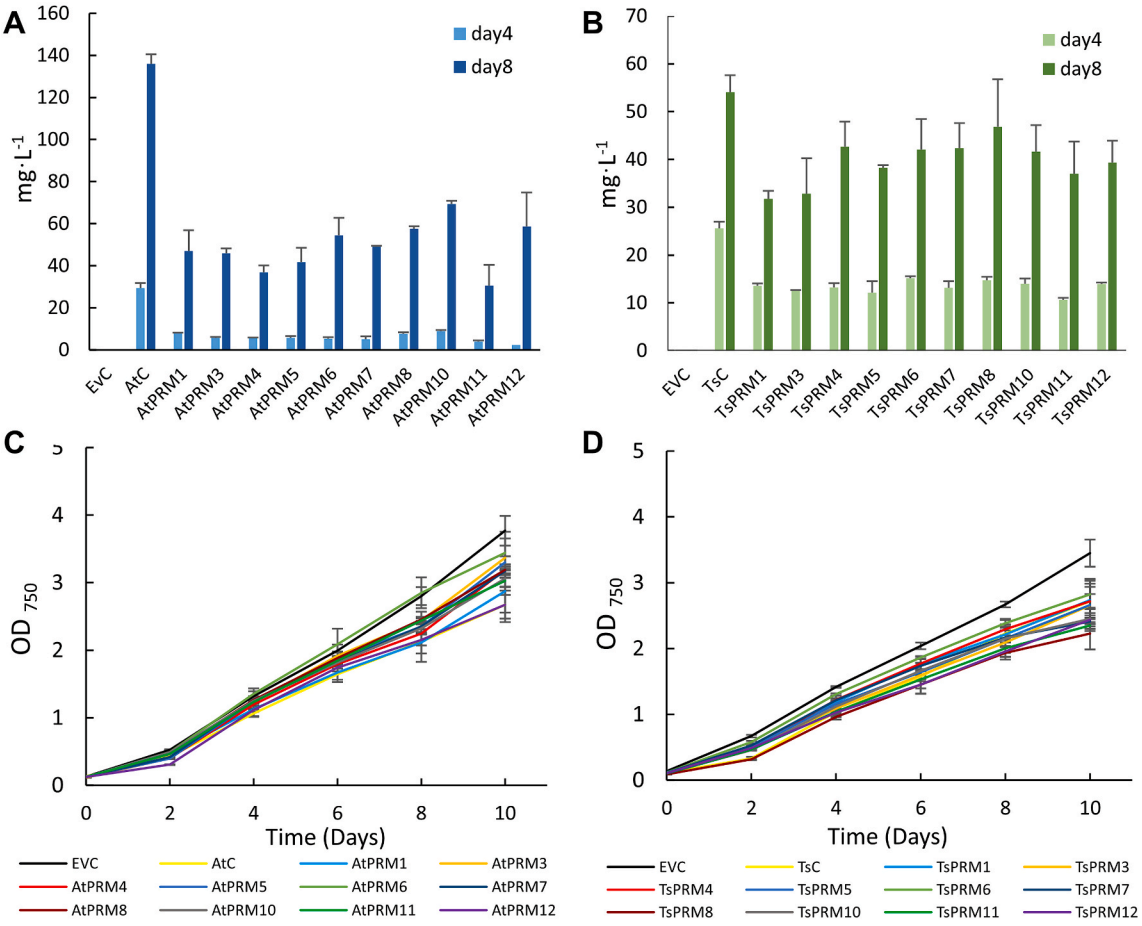

Fig. 6. Productivity and growth of AtPRMs and TsPRMs during shake flasks cultivation. **A** Comparison of *t*CA production in ten AtPRM variants, TsC and EVC strains. **B** Comparison of *p*Cou production in ten TsPRM variants, TsC and EVC strains. Samples were taken from the growth medium at day four and day eight. The values are the means of three biological replicates and two technical replicates, error bars represent the standard deviation of three biological replicates. **C** Growth curves of EVC, AtC and AtPRMs during 10 days. **D** Growth curves of EVC, TsC and TsPRMs during 10 days. Error bars represent standard deviation of three biological replicates.

*t*CA and *p*Cou similar to other AtPRMs or TsPRMs (Fig. 6A and B).

We further tested the productivity of AtPRM and TsPRM strains during high-density cultivation. As for the experiments with Phe production in PRMs, the HDC conditions allowed us to identify strains with different productivity patterns. Similarly to the shake flasks experiments, the *t*CA productivity normalized to OD_{750} was lower compared to that in the AtC control strain by nearly 4-6 times for all PRMs tested with exception of AtPRM8 (Fig. 7A), which demonstrated more than 1.5

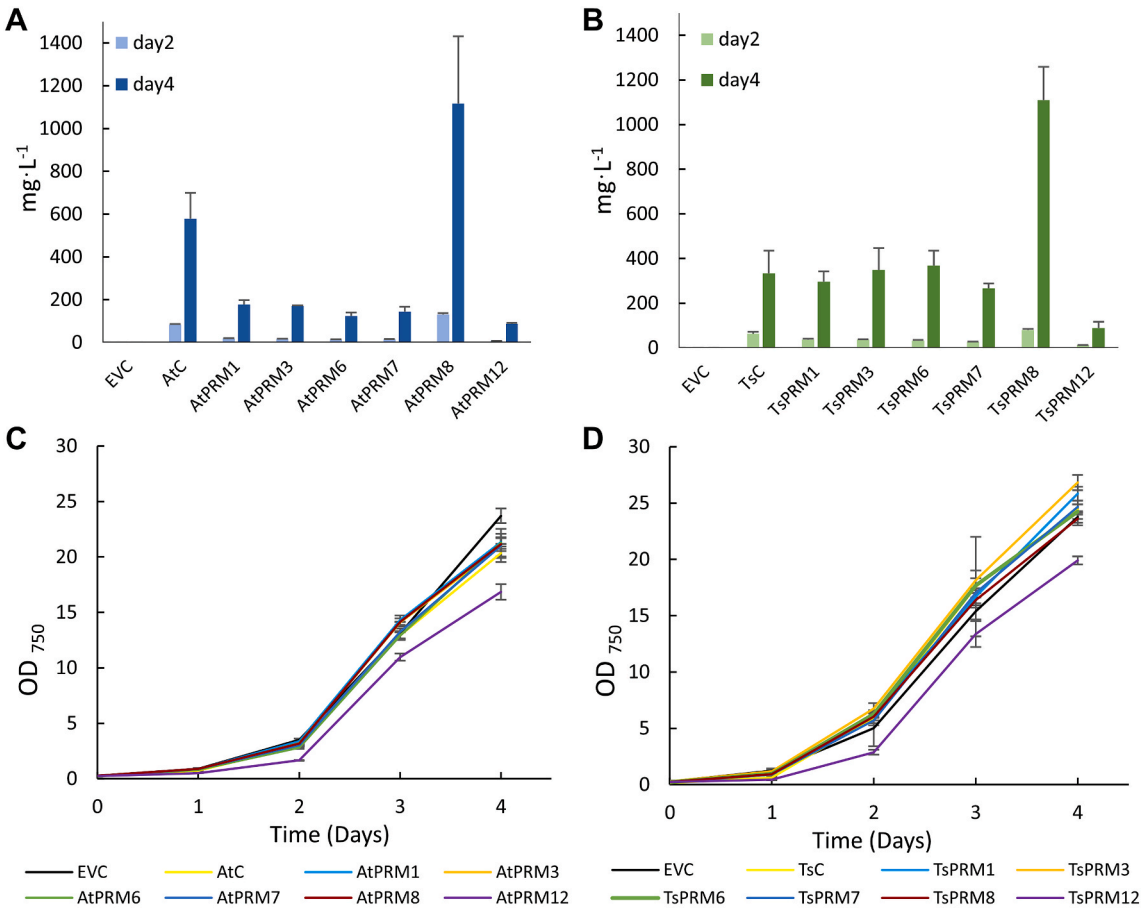

Fig. 7. Productivity and growth of AtPRMs and TsPRMs during high-density cultivation. **A** Comparison of *t*CA production in ten AtPRM variants, AtC and EVC strains. **B** Comparison of *p*Cou production in ten TsPRM variants, TsC and EVC strains. Samples were taken from the growth medium at day two and day four. The values are the means of three biological replicates and two technical replicates, error bars represent the standard deviation of three biological replicates. **C** Growth curves of EVC, AtC and AtPRMs during four days. **D** Growth curves of EVC, TsC and TsPRMs during four days. Error bars represent standard deviation of three biological replicates.

times productivity improvement at the last day of cultivation (52.7 ± 15 mg L^{-1}·OD_{750}^{-1} and 1116.7 ± 314 mg L^{-1} final titer). The overexpression of TAL in the PRM background strains resulted in nearly similar *p*Cou production compared to control strain TsC, with the exception of TsPRM8, which reached more than 3 times higher specific productivity with a titer of 47.1 ± 7 mg L^{-1}·OD_{750}^{-1} at day four of the HDC experiment, corresponding to 1108.8 ± 150 mg L^{-1} (Fig. 7B). Moreover, TsPRM8 also accumulated 18 ± 3 mg L^{-1} of Phe at the second day, whereas on day four the Phe concentration decreased to 1.1 ± 0.3 mg L^{-1} in the growth medium (data not shown). Traces of *t*CA were detected in TsPRMs during high-density cultivation; however, its concentration was below the quantification limit for all tested strains except when in TsPRM8 it reached 7.9 ± 2 mg L^{-1} on the last day of HDC cultivation (data not shown). Unlike the HDC data obtained for PRMs, where the low specific productivity might be due to the re-uptake of Phe from the media, secreted *t*CA and *p*Cou by AtPRM and TsPRM variants are not metabolized, and thus the lower productivity is unlikely to be related to the reuptake of these compounds.

3.4. Whole genome sequencing of PRMs

To identify the mutations that lead to the above-described phenotypes, the genomic DNA of PRM1, PRM8 and PRM12 was sequenced. The mutations in PRMs were determined with respect to re-sequenced *Synechocystis* WT, which was used as a reference genome to PRMs. The mapping results were compared to a reference genome *Synechocystis* sp. PCC6803 GT-Kazusa (NC_000911) (Kaneko et al., 1996) and showed 100% coverage for WT and sequenced PRMs. Segregated mutations present simultaneously in WT and PRM variants are summarized in Table S2. In total, there were 26 segregated mutations detected including single nucleotide polymorphism (SNP), deletions and insertions resulting in missense, silent and nonsense mutations or frame shifts, which all could be a result of a long-term laboratory acclimatization of WT *Synechocystis*. Four fully segregated mutations consistent among three PRMs variants but absent in WT were identified in genes *sll0934*, *slr1916*, *sll1995* and a single nucleotide substitution in a non-coding region (Table 2).

The *ccmA* (*sll0934)* gene was previously annotated as a carboxysome formation protein (Ogawa et al., 1994), whereas the same locus was predicted to encode DAHPS (according to KEGG) in *Synechocystis*. The DAHPS enzyme family shows diverse sequence variation due to small domains, additional to the catalytic core, that are involved in the allosteric regulation of DAHPS activity. DAHPS are divided into two distinct homology classes based on size and sequence similarity (types Iα, Iβ, and II) (Subramaniam et al., 1998). Based on sequence similarity, DAHPS from *Synechocystis* (*Syn*DAHPS) belongs to the Iβ family. As described for DAHPS from *Thermotoga maritima* (*Tma*DAHPS) (Shumilin et al., 2004), the Iβ family enzymes harbor an additional regulatory ferredoxin-like (FL) domain fused to the N-terminus of the catalytic core, which was demonstrated to be responsible for allosteric control. Binding of an effector molecule (Tyr in case of *Tma*DAHPS) between two diagonally opposed N-terminal FL domains of a homotetramer causes significant conformational rearrangements of the FL domains, forming a closed structure that occludes the active site. Truncation of the FL domain

Table 2
List of mutations identified in sequenced PRMs.

Strain	Location	Nucleotide change	AA change	Result	Locus	Enzyme
PRM1	206583	G → GTGAGGAGATT		Insertion	Non-coding region	
PRM1	335427	A → C	Val 66 Gly	AA change	*ccmA*	DAHP synthase
PRM8	335618	G → T	Ile 2 Lys	AA change	*ccmA*	DAHP synthase
	335619	A → T	DEL 12bp (7%)			
PRM12	335607-335619	TTCATGACGACGA → T	Deletion of AA 2,3,4,5	Deletion	*ccmA*	DAHP synthase
PRM 1,8,12	619742	C → T	Pro 42 Leu	AA change	*slr1916*	Probable esterase
PRM 1,8,12	1642069	G → GA	Glu 47 *	Frame shift and early stop codon	*sll1995*	Probable glycosyltranferase
PRM 1,8,12, WT (10%)	2084334	T → C			Non-coding region	
PRM12	2467257	G → T (50%)	Ala 359 Asp	AA change	*clpC*	ATP-dependent Clp protease regulatory subunit
PRM1	3138609	G → A			Non-coding region	-5 upstream of *sll0737*
PRM8	3224173	A → T (22%)			trnT-GGU	Threonine tRNA
	3224187	T → A (78%)				
	3224194	A → G (21%)				
	3224195	C → A (79%)				

resulted in an enzyme variant which is completely insensitive to allosteric inhibition, while retaining catalytic activity (Cross et al., 2011).

The mutations that occurred in *ccmA* in the sequenced PRMs involve one amino acid substitution in PRM1 (Val66Gly) and PRM8 (Ile2Leu), and the deletion of the first four amino acids in PRM12 (Ile2, Val3, Val4, Met5). A not fully segregated (12%) deletion of the same four amino acids also occurred in PRM8. To investigate these sequences in the remaining PRMs, we amplified the *ccmA* locus from genomic DNA of the PRMs and sequenced the amplicons. The results showed that PRM1-7 acquired the Val66Gly substitution, whereas in PRM10 and PRM11 an insertion of 10aa is present (Lys30–Val38, Ile39) duplicating the sequence Lys30 – Val38 (data not shown). Based on the sequence similarity of *Syn*DAHPS to structural homologues (Fig. S3), the Val66 of *Syn*DAHPS seems to be conserved and corresponds to the Val-65 of the *Tma*DAHPS flexible linker region, which was shown to be responsible for the deviation of the main chain of FL domain upon binding of Tyr (Cross et al., 2011). Thus, Val66Gly substitution in this region, plausibly, restricts the rearrangement of FL regulatory domain in *Syn*DAHPS in the presence of Phe effector molecule. The mutations at the N-terminal region (PRM8-PRM12) of the regulatory domain might affect the interaction of the opposite domains, which possibly could prevent effective Phe capturing and, as a consequence, the rearrangement of the protein in a “closed form”. To summarize, several different mutations that appeared in PRMs target the regulatory FL domain of DAHPS and likely affect binding of Phe to the allosteric site, thereby relieving allosteric inhibition of *Syn*DAHPS by Phe. In line with this, the decreased *t*CA and *p*Cou productivity in PRM background compared to WT background strains could be explained by lower catalytic activity of such deregulated DAHPS, suggesting a tradeoff between activity and loss of allosteric control. In the case of PRM8 and PRM8 based strains that demonstrate superior production rates of Phe, *t*CA and *p*Cou during HDC experiments, the Ile2Leu substitution supposedly does not negatively affect the activity of DAHPS enzyme. However, further studies would be necessary to investigate the activity and allosteric regulation of *Syn*DAHPS. In recent interaction proteomics studies, interaction of *Synechocystis* CcmA with Phe was demonstrated (Sporre et al., 2022), and it would be interesting in a future study to investigate whether the interaction is abolished in our CcmA mutants.

For the mutations in *sll1995*, PRMs 1, 8 and 12 all contained one nucleotide insertion at Glu47 position, causing a frameshift with an introduction of an early stop codon resulting in protein truncation. Amplification and sequencing of the *sll1995* locus confirmed that the insertion at Glu47 is present in all PRMs. *sll1995* encodes an unknown protein with probable glycosyltransferase activity which has not been characterized, making it difficult to predict the potential effect of deactivation of this protein in *Synechocystis*.

In *slr1916*, a mutation present in the genome of sequenced PRMs involved a single codon substitution that results in a Pro42Leu substitution. As for the other conserved mutations, the *slr1916* locus was amplified from genomic DNA of the other PRMs and sequencing revealed that all PRMs contained the same Pro42Leu mutation. Slr1916 is annotated as a probable esterase, and was recently demonstrated to have chlorophyll dephytylase degradation activity *in vitro*, however the functional role of this enzyme has not been fully addressed (Chen et al., 2021), and the absence of a crystal structure makes it difficult to predict whether Pro42Leu causes changes of protein functionality. Proposedly, Slr1916 plays a global redox regulatory role rather than solely a chlorophyll degradation function (Chen et al., 2021), making the appearance of a mutation in this gene in PRMs intriguing. Mutations occurring in the *slr1916* gene have been reported in several studies, appearing also in the re-sequenced GT-T substrain of WT *Synechocystis* sp. PCC 6803 (Koskinen et al., 2023). It has been shown that *slr1916* and *pmgA* knock-out mutants are glucose sensitive under high light (Ozaki et al., 2007), whereas the confirmed loss-of-function mutation Cys53Tyr in *slr1916* correlated with a high light tolerance phenotype (Yoshikawa et al., 2021). Interestingly, in our study re-sequencing of WT as a reference genome showed one amino acid substitution in PmgA (Ser17Gly), which was absent in sequenced PRM mutants (Table S3). Furthermore, downregulation of the *slr1916* gene, as one of few others including *pmgA* identified in CRISPRi gene repression library, resulted in increased culture growth rates (Yao et al., 2020). Since the function of both *slr1916* and *pmgA* gene products was attributed to be involved in the modulation of photosystem stoichiometry although the exact mechanism is unknown (Ozaki et al., 2007), it is possible that the absence of *pmgA* mutation in PRMs was due to a reversion event and that this event and the appearance of the mutation in *slr1916* are linked.

The lower *t*CA productivity in the strains overexpressing PAL in PRMs compared to WT background indicates that the shikimate pathway regulation is more complex in these mutants than solely loss of feedback-inhibition sensitivity of DAHPS. Moreover, the different rates of Phe, *t*CA and *p*Cou accumulation in different PRM variants can correspond to a diverse set of mutations that appear as an adaptive mechanism in cells to overcome the selective pressure of supplemented Phe. This also means that for future engineering, there are likely to be more target genes and enzymes involved in the function and regulation of aromatic amino acid biosynthesis in *Synechocystis* than previously identified.

4. Conclusions

In this project, following the aim to develop cyanobacteria as a biotechnological platform for renewable, solar-powered production of aromatic compounds, we have obtained laboratory-evolved mutants of *Synechocystis* sp. PCC 6803 by applying selective pressure of Phe. The resulting PRMs are able to secrete aromatic amino acids Phe and Tyr into the growth medium. The growth inhibition of *Synechocystis* by Phe was investigated, showing that the Phe consumption during growth inhibition is marginal and the timing of appearance of resistant colonies depends on the provided concentration of Phe. Comparative growth and production experiments showed that the PRM strains had similar specific production of Phe, with a maximum obtained level of 9.1 ± 0.7 mg $L^{-1}\cdot OD_{750}^{-1}$ for PRM10 after 8 days of photoautotrophic growth. High-density cultivation of PRMs resulted in lower specific production than in shake flasks, with the exception of one mutant, PRM8, which reached the highest specific production of 24.9 ± 7 mg $L^{-1}\cdot OD_{750}^{-1}$ or 610 ± 196 mg L^{-1} after four days.

In order to determine whether the PRMs can improve the *t*CA and *p*Cou production compared to the WT background, we overexpressed PAL and TAL in the mutant strains. However, the *t*CA productivity dropped nearly four times for some AtPRMs compared to the AtC control strain. The *p*Cou production, on the other hand, was in a similar range between TsPRMs and TsC. The high-density cultivation of AtPRMs and TsPRMs demonstrated the same production pattern relative to the corresponding WT background strain as in shake flasks experiment, except AtPRM8 and TsPRM8. Both these strains reached higher specific production than the corresponding control strains with 52.7 ± 15 mg $L^{-1}\cdot OD_{750}^{-1}$ *t*CA for AtPRM8 and 47.1 ± 7 mg $L^{-1}\cdot OD_{750}^{-1}$ *p*Cou for TsPRM8, and a volumetric production of above 1 g L^{-1} in four days for both strains.

Whole genome sequencing revealed that PRMs acquired mutations in the *ccmA* gene that encodes DAHPS. Although among 10 PRMs mutations were distinct, all of them appeared in a regulatory domain of the enzyme supposedly causing the loss of allosteric sensitivity. Allosteric deregulation, on the other hand, might have as well affected the activity of mutated DAHPS, which resulted in the lower productivity titers of *t*CA and *p*Cou in the PRM-based strains. The data obtained in this study provides highly important information for understanding the understudied cyanobacterial metabolism and regulation of aromatic amino acids synthesis. The combination of laboratory-evolved mutants and targeted metabolic engineering can be a powerful tool to develop new microbial platforms reaching high production rates of various industrially relevant products in cyanobacteria.

Credit author statement

Kateryna Kukil: Conceptualization, Methodology, Investigation, Writing - Original draft, review & editing, Visualization. **Elias Englund:** Methodology, Investigation, Writing - Review & editing. **Nick Crang:** Methodology, Investigation, Writing - Review & editing. **Elton P. Hudson:** Supervision, Writing - Review & editing. **Pia Lindberg:** Conceptualization, Supervision, Writing - Original draft, review & editing.

Data availability

Data will be made available on request.

Acknowledgments

This work was supported by Formas [Grant No. 2016-01325], the Nord-Forsk NCoE program “NordAqua” [Project Number 82845], Novo Nordisk Fonden (Grant. No. NNF20OC0061469), and the Swedish Foundation for Strategic Research (Grant No. FFF20-0027).

Appendix A. Supplementary data

Supplementary data to this article can be found online at https://doi.org/10.1016/j.ymben.2023.06.014.

References

Brey, L.F., Włodarczyk, A.J., Thøfner, J.F.B., Burow, M., Crocoll, C., Nielsen, I., Nielsen, A.J.Z., Jensen, P.E., 2020. Metabolic engineering of *Synechocystis* sp. PCC 6803 for the production of aromatic amino acids and derived phenylpropanoids. Metab. Eng. 57, 129–139.

Chen, G.E., Hitchcock, A., Mareš, J., Gong, Y., Tichý, M., Pilný, J., Kovářová, L., Zdvihalová, B., Xu, J., Hunter, C.N., 2021. Evolution of Ycf54-independent chlorophyll biosynthesis in cyanobacteria. Proc. Natl. Acad. Sci. USA 118 (10), e2024633118.

Cross, P.J., Dobson, R.C., Patchett, M.L., Parker, E.J., 2011. Tyrosine latching of a regulatory gate affords allosteric control of aromatic amino acid biosynthesis. J. Biol. Chem. 286 (12), 10216–10224.

Dehm, D., Krumbholz, J., Baunach, M., Wiebach, V., Hinrichs, K., Guljamow, A., Tabuchi, T., Jenke-Kodama, H., Sussmuth, R.D., Dittmann, E., 2019. Unlocking the spatial control of secondary metabolism uncovers hidden natural product diversity in *Nostoc punctiforme*. ACS Chem. Biol. 14 (6), 1271–1279.

Deshpande, A., Vue, J., Morgan, J., 2020. Combining random mutagenesis and metabolic engineering for enhanced tryptophan production in *Synechocystis* sp. strain PCC 6803. Appl. Environ. Microbiol. 86 (9), e02816, 02819.

Dienst, D., Wichmann, J., Mantovani, O., Rodrigues, J.S., Lindberg, P., 2020. High density cultivation for efficient sesquiterpenoid biosynthesis in *Synechocystis* sp. PCC 6803. Sci. Rep. 10 (1), 1–16.

Ducat, D.C., Avelar-Rivas, J.A., Way, J.C., Silver, P.A., 2012. Rerouting carbon flux to enhance photosynthetic productivity. Appl. Environ. Microbiol. 78 (8), 2660–2668.

Gao, E.-B., Kyere-Yeboah, K., Wu, J., Qiu, H., 2021. Photoautotrophic production of p-Coumaric acid using genetically engineered *Synechocystis* sp. Pasteur Culture Collection 6803. Algal Res. 54, 102180.

Grund, M., Jakob, T., Wilhelm, C., Bühler, B., Schmid, A., 2019. Electron balancing under different sink conditions reveals positive effects on photon efficiency and metabolic activity of *Synechocystis* sp. PCC 6803. Biotechnol. Biofuels 12 (1), 1–14.

Hall, G.C., Jensen, R.A., 1980. Enzymological basis for growth inhibition by L-phenylalanine in the cyanobacterium *Synechocystis* sp. 29108. J. Bacteriol. 144 (3), 1034–1042.

Ivleva, N.B., Golden, S.S., 2007. Protein extraction, fractionation, and purification from cyanobacteria. Circadian rhythms 365–373. Springer.

Jiao, W., 2021. Computational investigations of allostery in aromatic amino acid biosynthetic enzymes. Biochem. Soc. Trans. 49 (1), 415–429.

Kaneko, T., Sato, S., Kotani, H., Tanaka, A., Asamizu, E., Nakamura, Y., Miyajima, N., Hirosawa, M., Sugiura, M., Sasamoto, S., 1996. Sequence analysis of the genome of the unicellular cyanobacterium *Synechocystis* sp. strain PCC6803. II. Sequence determination of the entire genome and assignment of potential protein-coding regions. DNA Res. 3 (3), 109–136.

Koskinen, S., Kurkela, J., Linhartová, M., Tyystjärvi, T., 2023. The genome sequence of *Synechocystis* sp. PCC 6803 substrain GT-T and its implications for the evolution of PCC 6803 substrains. FEBS Open Bio.

Kukil, K., Lindberg, P., 2022. Expression of phenylalanine ammonia lyases in *Synechocystis* sp. PCC 6803 and subsequent improvements of sustainable production of phenylpropanoids. Microb. Cell Factories 21 (1), 8.

Labarre, J., Thuriaux, P., Chauvat, F., 1987. Genetic analysis of amino acid transport in the facultatively heterotrophic cyanobacterium *Synechocystis* sp. strain 6803. J. Bacteriol. 169 (10), 4668–4673.

Lippi, L., Bähr, L., Wüstenberg, A., Wilde, A., Steuer, R., 2018. Exploring the potential of high-density cultivation of cyanobacteria for the production of cyanophycin. Algal Res. 31, 363–366.

Moschny, J., Lorenzen, W., Hilfer, A., Eckenstaler, R., Jahns, S., Enke, H., Enke, D., Schneider, P., Benndorf, R.A., Niedermeyer, T.H., 2020. Precursor-directed biosynthesis and fluorescence labeling of clickable microcystins. J. Nat. Prod. 83 (6), 1960–1970.

Ogawa, T., Marco, E., Orus, M.I., 1994. A gene (*ccmA*) required for carboxysome formation in the cyanobacterium *Synechocystis* sp. strain PCC6803. J. Bacteriol. 176 (8), 2374–2378.

Ozaki, H., Ikeuchi, M., Ogawa, T., Fukuzawa, H., Sonoike, K., 2007. Large-scale analysis of chlorophyll fluorescence kinetics in *Synechocystis* sp. PCC 6803: identification of the factors involved in the modulation of photosystem stoichiometry. Plant Cell Physiol. 48 (3), 451–458.

Quintero, M.J., Montesinos, M.L., Herrero, A., Flores, E., 2001. Identification of genes encoding amino acid permeases by inactivation of selected ORFs from the *Synechocystis* genomic sequence. Genome Res. 11 (12), 2034–2040.

Rao, S.R., Ravishankar, G., 2002. Plant cell cultures: chemical factories of secondary metabolites. Biotechnol. Adv. 20 (2), 101–153.

Rodrigues, J.S., Lindberg, P., 2021. Metabolic engineering of *Synechocystis* sp. PCC 6803 for improved bisabolene production. Metabol. Eng. Commun. 12, e00159.

Shumilin, I.A., Bauerle, R., Wu, J., Woodard, R.W., Kretsinger, R.H., 2004. Crystal structure of the reaction complex of 3-deoxy-D-arabino-heptulosonate-7-phosphate synthase from *Thermotoga maritima* refines the catalytic mechanism and indicates a new mechanism of allosteric regulation. J. Mol. Biol. 341 (2), 455–466.

Sporre, E., Karlsen, J., Schriever, K., Samuelsson, J.A., Janasch, M., Strandberg, L., Kotol, D., Zeckey, L., Piazza, I., Syrén, P.-O., Edfors, F., Hudson, E.P., 2022.

Metabolite interactions in the bacterial Calvin cycle and implications for flux regulation. bioRxiv. https://doi.org/10.1101/2022.03.15.483797.
Sprenger, G.A., 2006. Aromatic Amino Acids. Amino Acid Biosynthesis - Pathways, Regulation and Metabolic Engineering. Springer, pp. 93–127.
Stanier, R., Cohen-Bazire, G., 1977. Phototrophic prokaryotes: the cyanobacteria. Annu. Rev. Microbiol. 31 (1), 225–274.
Subramaniam, P.S., Xie, G., Xia, T., Jensen, R.A., 1998. Substrate ambiguity of 3-deoxy-D-manno-octulosonate 8-phosphate synthase from *Neisseria gonorrhoeae* in the context of its membership in a protein family containing a subset of 3-deoxy-D-arabino-heptulosonate 7-phosphate synthases. J. Bacteriol. 180 (1), 119–127.
Tamagnini, P., Troshina, O., Oxelfelt, F., Salema, R., Lindblad, P., 1997. Hydrogenases in *Nostoc* sp. strain PCC 73102, a strain lacking a bidirectional enzyme. Appl. Environ. Microbiol. 63 (5), 1801–1807.
Ververidis, F., Trantas, E., Douglas, C., Vollmer, G., Kretzschmar, G., Panopoulos, N., 2007. Biotechnology of flavonoids and other phenylpropanoid-derived natural products. Part I: chemical diversity, impacts on plant biology and human health. Biotechnol. J.: Healthcare Nutrition Technology 2 (10), 1214–1234.
Vogt, T., 2010. Phenylpropanoid biosynthesis. Mol. Plant 3 (1), 2–20.
Yadav, V., Wang, Z., Wei, C., Amo, A., Ahmed, B., Yang, X., Zhang, X., 2020. Phenylpropanoid pathway engineering: an emerging approach towards plant defense. Pathogens 9 (4), 312.
Yao, L., Shabestary, K., Björk, S.M., Asplund-Samuelsson, J., Joensson, H.N., Jahn, M., Hudson, E.P., 2020. Pooled CRISPRi screening of the cyanobacterium *Synechocystis* sp PCC 6803 for enhanced industrial phenotypes. Nat. Commun. 11 (1), 1666.
Yoshikawa, K., Ogawa, K., Toya, Y., Akimoto, S., Matsuda, F., Shimizu, H., 2021. Mutations in *hik26* and *slr1916* lead to high-light stress tolerance in *Synechocystis* sp. PCC6803. Commun. Biol. 4 (1), 343.